Available online at www.sciencedirect.com
SCIENCE DIRECT®
Carbohydrate Polymers 53 (2003) 145–153
Carbohydrate Polymers
www.elsevier.com/locate/carbpol

A gelation mechanism depending on hydrogen bond formation in regioselectively substituted *O*-methylcelluloses

Yuka Sekiguchi[a,1], Chie Sawatari[a], Tetsuo Kondo[b,*]

[a]*Graduate School of Electronic Science and Technology, Shizuoka University, 3-5-1 Johoku, Hamamatsu, Shizuoka 432-8011, Japan*
[b]*Forestry and Forest Products Research Institute (FFPRI), P.O. Box 16, Tsukuba Norin Kenkyu, Tsukuba, Ibaraki 305-8687, Japan*

Received 3 January 2002; revised 9 July 2002; accepted 1 August 2002

Abstract

This paper discusses how the hydrophobic interactions as well as hydrogen bonds contribute to thermally reversible gelation of aqueous solutions for *O*-methylcellulose. The gelation behavior of a series of regioselectively substituted 2,3-di-*O*-methylcellulose (2,3MC-*n*: $n = 1-3$) differed from that for randomly substituted *O*-methylcellulose (R-MC). This was indicated by differential scanning calorimetry, near infrared spectroscopy (NIR) and small angle X-ray scattering. The formation of hydrogen bonds in 2,3MC-*n* and R-MC solutions was also determined by the curve fitting results of OH bands in NIR spectra. This method proved the presence of the intermolecular hydrogen bonds between the cellulosic samples and water. As a result, the gelation of the 2,3MC-*n* and R-MC solutions may be caused by cooperation of the hydrophobic interaction among methyl substituents with the intermolecular hydrogen bonds among hydroxyl groups at the C(6) position, which are dependent on the distribution of methyl groups.

Keywords: Gelation; *O*-methylcellulose; Hydrogen bond; Regioselectively substitution; FT-NIR; DSC

1. Introduction

The distribution of methyl and other substituents within an anhydroglucose unit as well as along the molecular chain is considered to be an important factor determining the physicochemical properties of cellulose derivatives. Chemical modifications of cellulose for commercial applications are generally conducted under heterogeneous conditions. Such heterogeneous reactions cause a variety of introduction of the substituents within an anhydroglucose unit as well as along the molecular chain in cellulose derivatives, which also causes variable physicochemical properties for the products. When cellulose derivatives are composed of a homogeneous chemical structure, their physicochemical properties may be directly predicted (Takaragi, Fujimoto, Miyamoto, & Inagaki, 1987).

Recently, we succeeded in preparing *O*-alkylcellulose derivatives having a systematically controlled distribution of substituents and degree of substitution (DS) (Kondo, 1993; Kondo & Gray, 1991, 1992). The use of these derivatives, 2,3-di-*O*-methylcellulose (Kondo & Gray, 1991), 6-*O*-methylcellulose (Kondo, 1993), and tri-*O*-methylcellulose (Kondo & Gray, 1992) was expected to clarify the correlation between the physicochemical properties and the distribution of substituents in terms of hydrogen bonding formation. The distribution of substituents was found to influence the inter- and intramolecular hydrogen bonding formation, which contributes to the solubility (Kondo, 1997a), gelation (Itagaki, Takahashi, Natsume, & Kondo, 1994; Itagaki, Tokai, & Kondo, 1997), liquid crystallization (Kondo & Miyamoto, 1998), crystallization, and chemical reactions of hydroxyl groups (Kondo, 1997a) in cellulose derivatives. The distribution of substituents also affects the susceptibility of the cellulose derivatives to enzymatic degradation (Kondo & Nojiri, 1994; Nojiri & Kondo, 1996).

Commercial *O*-methylcellulose is widely used, for example, as a thickener for foods and cosmetics, a coating material for medicines, and a binder for ceramic and cement. Aqueous solutions of *O*-methylcellulose are also known to form a gel on heating and then revert to the solution on cooling. The thermoreversible gelation

* Corresponding author. Tel.: +81-92-642-2997; fax: +81-92-642-2997.
E-mail address: tekondo@agr.kyushu-u.ac.jp (T. Kondo).
[1] Present Address: Graduate School of Bioresources and Bioenvironmental Science, Kyushu University, 6-10-1, Hokozaki, Fukuoka 812-8581, Japan.

0144-8617/03/$ - see front matter © 2003 Elsevier Science Ltd. All rights reserved.
doi:10.1016/S0144-8617(03)00050-X

mechanism of *O*-methylcellulose solution has been proposed (Kato, Yokoyama, & Takahashi, 1978; Sarkar, 1979, 1995; Suzuki, Taniguchi, & Enomoto, 1972), but is not completely clarified. Recently, Hirren, Desbrieres, and Rinaudo (1997) and Vigouret, Rinaudo, and Desbrieres (1996) reported the effect of the distribution of substituents on the gelation of *O*-methylcellulose. In this paper, we particularly focus on the influence of inter- and intramolecular hydrogen bonds. The gelation behavior was investigated using *O*-methylcellulose with a systematically controlled distribution of substituents and DS. An aqueous solution of the commercial sample with heterogeneous distribution of substituents was also compared in terms of the gelation process.

2. Experimental

2.1. Materials

Two types of *O*-methylcellulose used were as follows; one was *O*-methylcellulose sample series (the DS range of 1.0–1.8 and soluble in water) which were regioselectively methylated only at the C(2) and C(3) positions including also non-methylated hydroxyl groups at the C(6) positions. The series of regioselectively substituted *O*-methylcellulose samples (2,3MC-*n*: $n = 1$–3, Fig. 1(A)) was prepared by multiple methylation of 6-*O*-triphenylmethylcellulose (6TC) as a starting material basically following the method reported previously (Kondo & Gray, 1991). The numbering of the sample corresponded to the repeating number of the methylation steps; for example, 2,3MC-1 indicates the single-methylated sample of 6TC. 'R-MC' was indicated as commercially available and randomly methylated *O*-methylcellulose (Fig. 1(B)) having blocky regions of either trimethyl glucose ether or non-methylated glucose sequences (Shin-Etsu Chemical Co.).

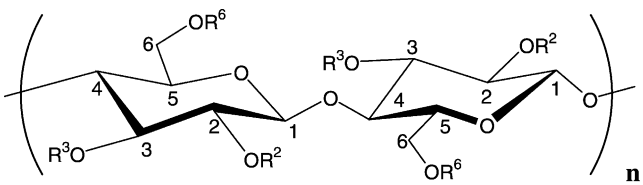

	R^2	R^3	R^6
(A) 2,3MC-n (n = 1-3)	CH_3 or H	CH_3 or H	H
(B) R-MC	CH_3 or H	CH_3 or H	CH_3 or H

Fig. 1. The chemical structures of the *O*-methylcellulose samples in this study.

The above samples were dissolved in water, and centrifuged at 15,000 rpm to remove insoluble impurities. The supernatant was isolated and dried at 50 °C. The dried samples were again dissolved in water at room temperature, and then kept mixing under the same condition for 24 h to assure a complete dissolution.

2.2. Characterization of O-methylcelluloses

HPLC analysis to obtain an average molecular weight for each sample was performed with a Shimadzu Chromatopac C-R7A equipped with a refractive index detector (Shimadzu RID 6A). The column was Shodex OHpac SB-800HQ (polymethacrylate: $8\phi \times 300$ mm). The eluent was 0.1 M $NaNO_3$, and the flow rate was 1 ml/min at 55 °C. A calibration curve was obtained based on a series of pullulan standards (8.53×10^5, 3.5×10^5, 1.86×10^5, 1.0×10^5, 4.8×10^4, 2.37×10^4, 1.22×10^4, 5.2×10^3, and 1.8×10^2 as an average molecular weight).

^{1}H–NMR spectra were measured with a JEOL-GX 400 FT-NMR spectrometer (400 MHz) at 15 °C, using D_2O as solvent with a concentration of ca. 1%. The spectra were recorded after 400 scans for R-MC and 40 scans for 2,3MC samples, respectively, which can provide clear enough spectra for analysis. The peak signals were assigned based on the previous report (Sekiguchi, Sawatari, & Kondo, 2002).

FT-mid IR spectra were recorded using a Perkin–Elmer FTIR spectrometer, Spectrum 1000. The wavenumber range was 4000–400 cm^{-1}; the data were collected after 32 scans of 2 cm^{-1} resolution. The film specimens used in this study were cast from water. They were then vacuum-dried at 60 °C for more than a week until the free water was believed to be completely removed. Thus, the IR frequencies due to hydroxyl groups (OH) were originated from the cellulose samples. Baseline correction in IR spectra was performed assuming that the intensity of absorbance is zero at the on and off set points of bands due to CO_2 (2340 cm^{-1}) and CH (2900 cm^{-1}) stretching vibration and at both ends of the measured range (4000 and 400 cm^{-1}). Curve fitting for the peak deconvolution of hydroxyl groups frequencies was performed using the GRAMS/386 'CurveFit' program. For the initial flexible parameter setting, the true shape of the peak of hydroxyl absorption bands was set to be a mixture of composition of Gaussian and Lorentzian. After calculations, the resultant line shapes were found to be all 100% Gaussian ones. The number of peaks involved in frequencies was determined using the second derivative IR spectra for the samples, in the range of 3700–3100 cm^{-1} (Kondo, 1997b). The calculations were repeated until a best fit was obtained with $R^2 > 0.999$, R : correlation factor.

2.3. Characterization of gels from O-methylcelluloses

Gelation behaviors of the aqueous sample solutions were observed in a water bath with a constant temperature. After

standing for the desired time, the solution was judged to become a gel in a vial when it lost fluidity.

DSC measurements were performed on 700 mg of the solutions using a Setaram micro DSC3 in a nitrogen atmosphere. An equal amount of distilled water was used as reference to obtain a flat base line. The heating scans were carried out in the temperature range of 25–90 °C at a rate of 1.0 or 0.1 °C/min. We used at least three sample specimens or more for the same series of measurements. For DSC and NIR, the curve shapes were reproducible. Deviation of the curves was within a minimum error range (1–2%).

FT-NIR spectra were measured using a Perkin–Elmer FTIR spectrometer, Spectrum 1000 equipped with a NIR light source, a KBr beam splitter and a DTGS detector. On measurements, the sample specimens were on a hot stage (Lincam TH-600PM) at the desired temperature and then scanned by NIR. The detailed procedure was as follows; the solution was poured into a borehole with 5 mm in diameter in the PET plate ($20\phi \times 0.5$ mm), and the PET plate was sandwiched between two plates of crystal of CaF_2 ($20\phi \times 1$ mm). The specimen thus prepared was set in the hot stage. The heating scans were carried out in the temperature range of 30–90 °C at a rate of 1.0 °C/min. The wavenumber range was 7800–400 cm^{-1}; the data were collected after 100 scans of 2 cm^{-1} resolution. Curve fitting for the peak in the range of 7400–6000 cm^{-1} was performed as described above.

Small angle X-ray scattering (SAXS) measurements were performed at the beam line #15A of photon Factory of the National Laboratory for High Energy Physics (Tsukuba, Japan). The wavelength used in this study was 1.506 Å. The sample was heated using a heating apparatus (Mettler Instrument FP89), and the temperature was kept at 65 °C for 60 min. The diffraction intensity along the meridianal direction was recorded using a dimensional position-sensitive proportional counter (PSPC, Rigaku, Tokyo, Japan).

3. Results and discussion

3.1. Characterization of O-methylcellulose films

Prior to characterization of gel states of the samples, *O*-methylcelluloses were characterized as films. The characteristics of the *O*-methylcellulose samples are summarized in Table 1. 2,3MC-*n* samples have partially methylated hydroxyl groups only at the C(2) and C(3) positions and all free hydroxyl groups at the C(6) positions. 2,3MC-1 (1a, 1b and 1c) samples have similar degree of substitution (DS) with different molecular weights. These were prepared by different duration periods for bubbling with HCl gas to remove the triphenylmethyl groups as a protective group at the C(6) position (Kondo & Gray, 1991). We should add that these methylation steps did not result in lowering of the molecular weight of the material; namely no depolymerization occurred. 2,3MC-*n* samples having DS < 1 or DS $= 2$ were not used in this study, because these samples were insoluble in water (Liu, Zhang, Takaragi, & Miyamoto, 1997).

Fig. 2 shows IR spectra of 2,3MC-*n* and R-MC dried films. These IR spectra were normalized at 1110 cm^{-1} attributed to C–O–C stretching within an anhydroglucose ring. As the DS increased, the larger the C–H stretching vibration region (3000–2800 cm^{-1}) in the IR spectra of these samples became, and the smaller the OH stretching region (3700–3000 cm^{-1}) was. The shape of OH stretching band in R-MC was different from those in 2,3-MC-*n* samples. The difference may depend on hydrogen bonding formation in cellulose derivatives. OH stretching bands in cellulose derivatives are assumed to be a combination of bands including not only the inter- and intramolecular hydrogen bonded hydroxyl groups, but also a small number of 'free' or non-hydrogen bonded hydroxyl groups (Kondo, 1997b).

By a curve fitting method for the IR spectrum in 2,3MC-1b film, the OH stretching absorption band was deconvoluted into three OH bands with peaks at 3590 (A), 3465 (B),

Table 1
Molecular weight and degree of substitution of methyl and hydroxyl groups in the *O*-methylcellulose samples

Samples	M_n[a]	DS in film				
		Total-DS(OMe)[b]	Total-DS(OH)[c]	Free-OH[d]	Intra-OH[d]	Inter-OH[d]
R-MC	279,300	1.60	1.40	–	–	–
2,3MC-1a	29,300	1.02	1.98	0.009	1.238	0.733
2,3MC-1b	18,100	1.05	1.95	0.014	1.121	0.815
2,3MC-1c	11,900	0.92	2.08	0.017	1.381	0.682
2,3MC-2b	17,700	1.28	1.72	0.025	0.988	0.707
2,3MC-3b	16,200	1.85	1.15	0.008	0.630	0.512

[a] M_n is molecular weight, and determined by HPLC.
[b] Total-DS(OMe) is the degree of substituted methyl groups, and determined by ^{1}H–NMR measurements.
[c] Total-DS(OH) is the degree of unsubstituted hydroxyl groups, and calculated by subtracting the degree of substituents methyl groups of total-DS(OMe) from 3.
[d] DS of free-, intra-, and inter-OH are calculated by multiplying DS of total-DS(OH) by the percentage of each area to that of the total area of the OH band.

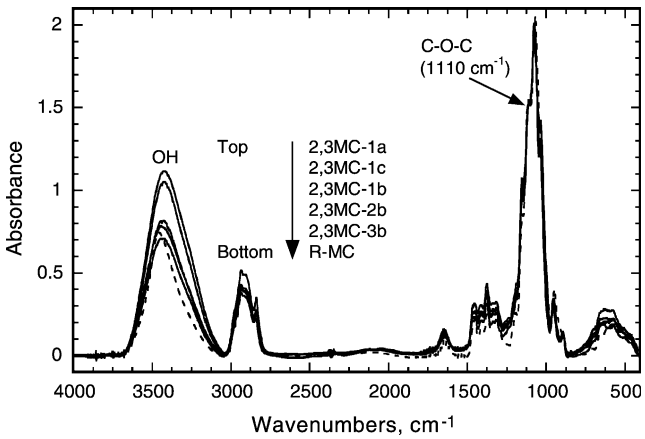

Fig. 2. IR spectra in the cast film of the *O*-methylcellulose samples.

and 3310 cm^{-1} (C), respectively (shown in Fig. 3). Two types of inter- and intramolecular hydrogen bonds can be involved in the pure cellulose film (Fig. 4(A)) and the 2,3-di-*O*-methylcellulose film (Fig. 4(B)) (Kondo, 1994, 1997a). In the present cases, as 2,3MC-*n* samples have partially methylated hydroxyl groups only at C(2) and C(3) positions, their cast films may have intramolecular hydrogen bonds engaged either between C(3)–OH and the adjacent ring oxygen or between C(6)–OH and C(2)–OCH_3. Kondo (1994, 1997a,b) reported that regioselectively substituted *O*-methylcelluloses such as 2,3-di-*O*-methylcellulose and 6-*O*-methylcellulose provide markedly sharper and narrower IR bands due to OH stretching frequencies when compared with cellulose having a diversity of inter- and intramolecular hydrogen bonds. It was also proposed that the sharper OH bands in the derivatives indicated specific hydrogen bonds; a single Gaussian band at 3460–3470 cm^{-1} in 6-*O*-methycellulose may be due to two of the almost identical intramolecular hydrogen bonds at the C(3) position engaged with adjacent ring oxygen and between C(2)–O*H* and *O*CH3 at the C(6) position. In the light of the above, the band B in Fig. 3 may be attributed to the intramolecular hydrogen bonds at the C(3) position, as well as to

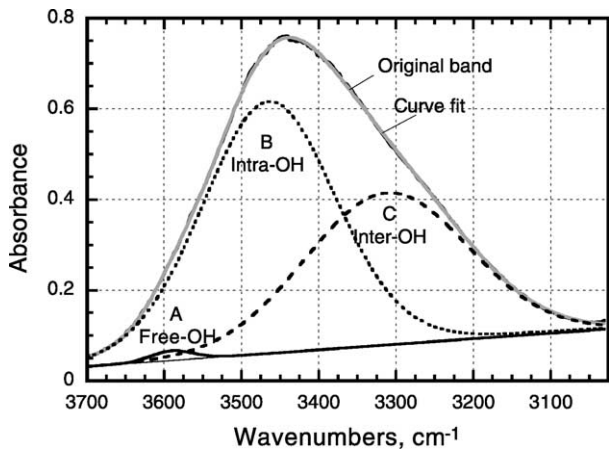

Fig. 3. Curve fitting and peak assignments for OH band of IR spectrum in the cast film of 2,3MC-1b.

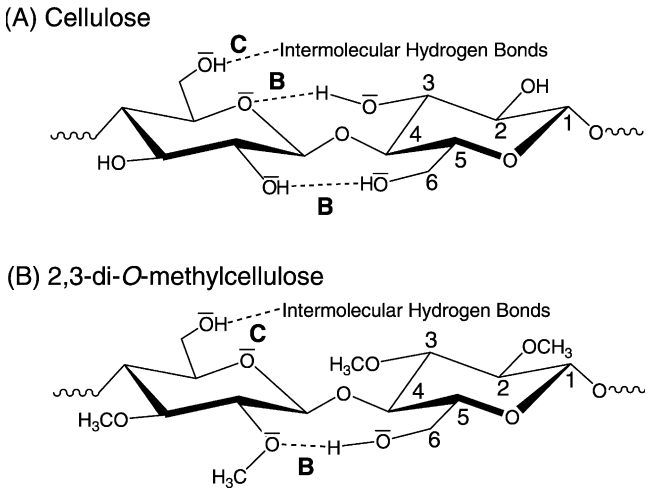

Fig. 4. Schematic representation of possible hydrogen bonds in cellobiose units of (A) cellulose and (B) 2,3-di-*O*-methylcellulose.

the intramolecular hydrogen bonds between the functional groups at the C(2) and C(6) positions. In general IR bands due to intermolecular hydrogen bonds appear at a lower wave number as a broader shape in comparison with those due to intramolecular hydrogen bonds. Thus, the band C may be due to the intermolecular hydrogen bonds at the C(6) positions. The band A may be due to remaining free hydroxyl groups at the C(2) position, which had escaped the methylation, or free hydroxyl groups at the C(6) position which were not involved in the intermolecular hydrogen bonds (Kondo, 1997b). The degree of substitution (DS) of the hydroxyl groups involved in the three types (A–C) of hydrogen bonding engagements as indicated in Figs. 3 and 4 was, therefore, calculated from the area of OH band, and listed in Table 1. Intramolecular hydrogen bonded hydroxyl groups in 2,3MC-1a and 2,3MC-1c were comparatively larger than those in the other 2,3MC-*n* samples.

3.2. Gelation of O-methylcellulose solutions

Aqueous solutions of 2,3MC-*n* and R-MC films became opaque on heating, and transformed to a gel on further heating. The gelation phenomena were time-dependent and thermally reversible with a hysteresis. Three solutions of the 2,3MC-*n* series as well as the R-MC solution formed gels. The phase diagram of these samples is shown in Fig. 5. The concentration of R-MC (molecular weight (M_n) = 280,000) required to form a gel was between 1 and 5 wt%, whereas that of the 2,3MC-*n*b series (M_n = 16,000–18,000) was between 20 and 25 wt%. This means the gelation of R-MC is attributed to hydrophobic interaction by trimethyl glucose sequences at a lower concentration (Kato et al., 1978). In the 2,3MC-1 series, only 2,3MC-1b, which was indicated to have the lowest intramolecular hydrogen bond in the film state as listed in Table 1, formed a gel, whereas neither 2,3MC-1a nor 2,3MC-1c formed a gel. Since the intramolecular hydrogen bonds between C(3)–OH and the adjacent

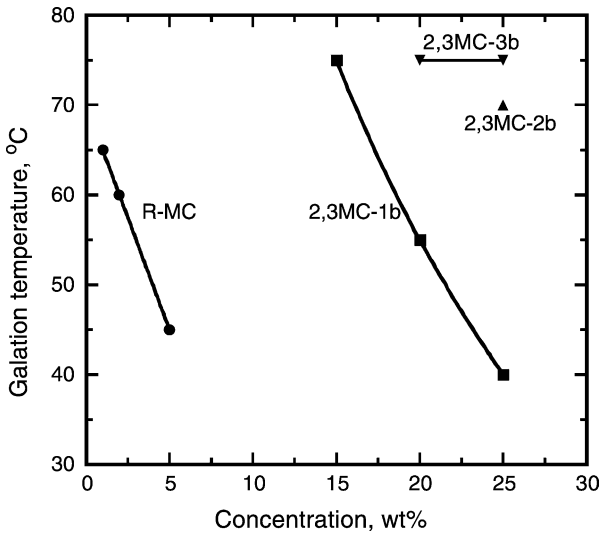

Fig. 5. Concentration dependence of critical gelation temperature of the *O*-methylcelluloses samples.

ring oxygen were suggested to be maintained in the *O*-methylcellulose solutions (Kondo, 1994, 1997a), the cellulose molecular chains of 2,3MC-1a and 2,3MC-1c must be less flexible than those of 2,3MC-1b. Thus, the lower flexibility may inhibit the gelation.

The 2,3MC-1b having the lowest DS of methyl groups in 2,3MC-*n*b series formed a gel at significantly lower temperatures than 2,3MC-2b and 2,3MC-3b. This indicates that the gelation mechanism of 2,3MC-*n*b samples may involve other interactions differing from the hydrophobic interaction that had been believed as a main initiation for a gel formation (Kato et al., 1978).

Fig. 6(a) illustrates the results of calorimetric experiments for solutions of 2,3MC-*n*b samples and R-MC. Two endothermic peaks (56 and 65 °C) were observed on heating R-MC. While the peak at 56 °C seemed to correspond to interactions involved with the highly substituted units, the peak at 65 °C may be due to the less substituted units (Hirren, Chevillard, Desbrières, Axelose, & Rinaudo, 1998). The heating DSC thermograms of the 2,3MC-*n*b solutions showed monotonic endothermic curves. The endothermic deviation of 2,3MC-1b slightly decreased at 60 °C, whereas those of 2,3MC-2b and 2,3MC-3b barely decreased at 75 °C. In spite of the slight changes, these phenomena correspond to the gelation phase diagram (Fig. 5), which shows that 2,3MC-1b formed a gel at lower temperatures when compared with 2,3MC-2b and 2,3MC-3b. As the gelation time of 1 wt% R-MC solution was 16 h, the DSC curve at a heating rate of 1.0 °C/min is considered to indicate thermal transition due to pre-gelation. In the calorimetric experiments carried out at a heating rate of 0.1 °C/min (Fig. 6(b)), the gelation was also observed. In R-MC solution, the endothermic curves between fast and slow rate scans were totally different. On the other hand, 2,3MC-1b solutions exhibited the similar endothermic curves in both the slower and the faster heating scans. This result also suggests that the gelation mechanism of 2,3MC-*n*b samples is different from that of R-MC. This difference was also shown in the gelation of *O*-methylcelluloses with homogeneous distribution of substituents prepared by another methylation method (Hirren et al., 1998; Nishimura, Donkai, & Miyamoto, 1997).

3.3. Characterization of O-methylcellulose solutions before and after gelation

We have focused on observing both behaviors of the OH groups in water and cellulose derivatives in separate ways

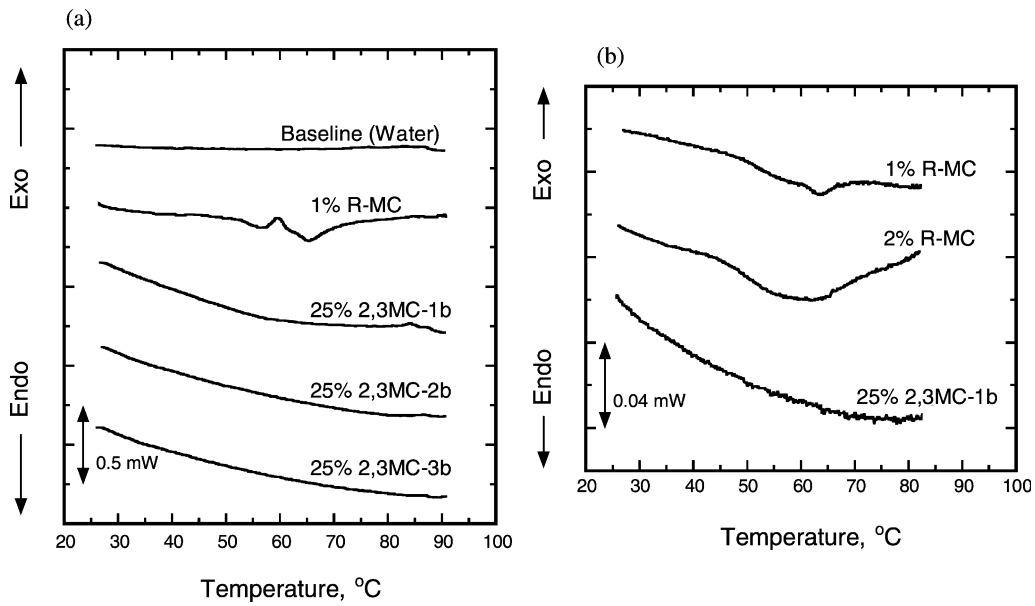

Fig. 6. Heating DSC thermograms of the *O*-methylcellulose solutions: Heating rates (a) 1.0 °C/min and (b) 0.1 °C/min. We used at least three sample specimens or more for the same series of measurements. The curve shapes were reproducible. Deviation of the curves was within a minimum error range (1–2%).

using near and mid IR, respectively. In mid-IR, it is not easy to obtain OH bands of water because the contribution of the OH in cellulose derivatives should be mostly overlapped. Thus, in measurements using mid-IR we used dried samples free of water to see the contribution of hydrogen bonds formed only in cellulose derivatives. On the other hand, near IR (NIR) analysis is rather easier to see the OH band of water although the interpretation is still difficult. Thus, the water structure in a gel state could be investigated using NIR. We should add that in fact it is hard to perform a correctly quantitative analysis on the water structure. Only a marked trend could be shown.

FT–NIR spectra of 2,3MC-1b and R-MC solutions were obtained to investigate the hydrogen bonding formation of water that may contribute to gel formation. Fig. 7 shows the OH band in the NIR region between 6000 and 7400 cm^{-1} that was assigned to $\nu_\delta + \nu_{as}$. The ν_δ and ν_{as} indicate the OH bending vibration and the OH anti-symmetric vibration, respectively (McCabe & Fisher, 1965, 1970). The OH absorption band was resolved into three component bands in the same manner as described for the film samples, where the peak tops were located at 7060, 6900, and 6660 cm^{-1}. These bands were assigned to the free water molecules (S0), water molecules with one OH engaged in hydrogen bonds (S1), and those with two OH engaged in hydrogen bonds (S2), respectively (Bujis & Choppin, 1963; Founés and Chaussidon, 1978).

The changes of S0, S1, and S2 areas due to water in 2,3MC-1b and R-MC solutions as a function of temperature, were listed in Table 2. At 30 °C where no gelation occurred, the areas of S1 of water in both 2,3MC-1b and R-MC solutions were larger than that in

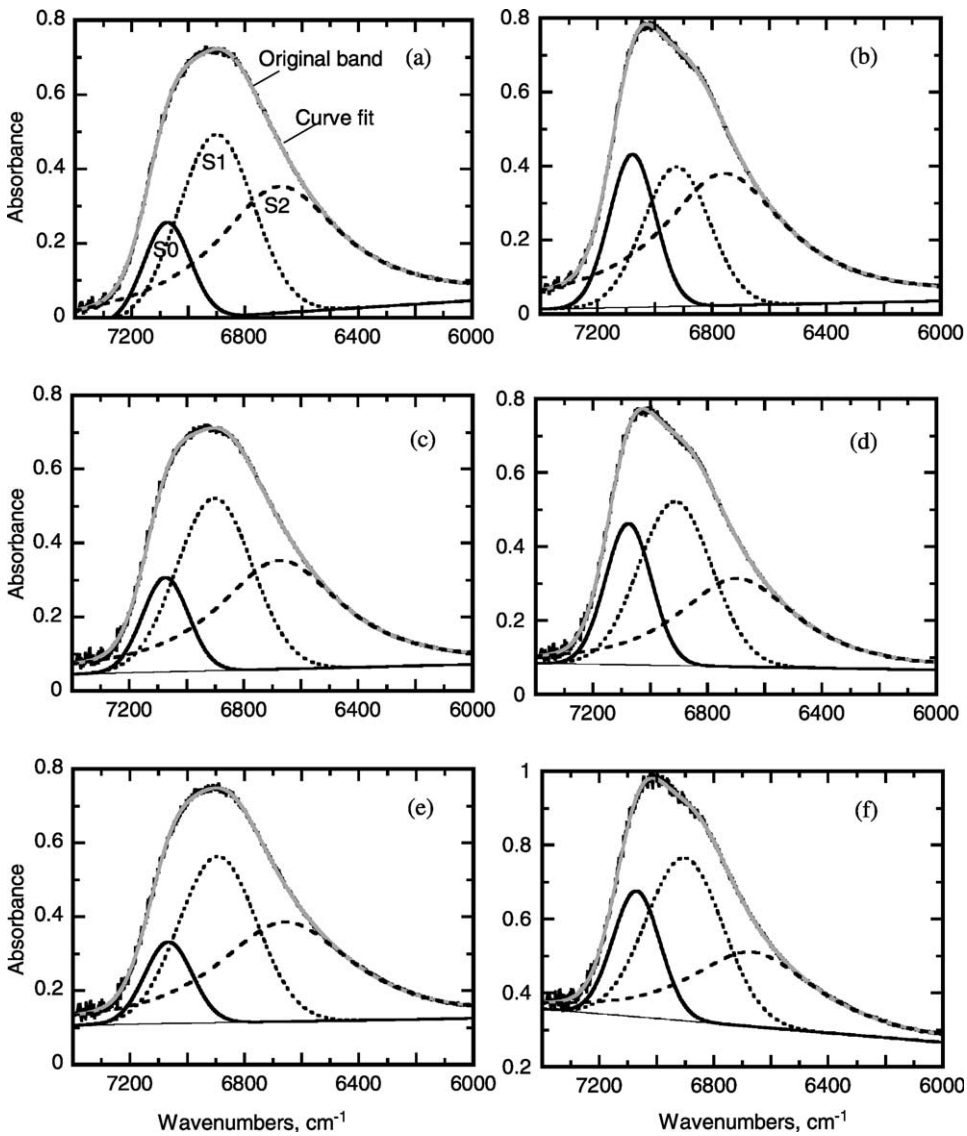

Fig. 7. Curve fitting and peak assignments for OH band ($\nu\delta + \nu_{as}$) of water in NIR spectra of (a) water at 30 °C, (b) water at 90 °C, (c) R-MC at 30 °C, (d) R-MC at 90 °C, (e) 2,3MC-1b at 30 °C, and (f) 2,3MC-1b at 90 °C. We used at least three sample specimens or more for the same series of measurements. The curve shapes were reproducible. Deviation of the curves was within a minimum error range (1–2%).

Table 2
The changes of S0, S1, and S2 areas in the OH bands of water in NIR spectra of the *O*-methylcellulose solutions on heating

Temperature (°C)	Solvent alone (water)			R-MC solution (2 wt%)			2,3MC-1b solution (25 wt%)		
	S0[a]	S1[a]	S2[a]	S0[a]	S1[a]	S2[a]	S0[a]	S1[a]	S2[a]
30	12.3	37.2	50.5	13.3	40.0	46.7	12.3	40.9	46.8
90	19.8	26.0	54.2	21.5	39.6	38.9	20.5	43.1	36.4

[a] S0, S1, and S2 indicate the water molecules with non-hydrogen bond, one hydrogen bond, and two hydrogen bonds, respectively.

solvent alone (pure water), whereas the areas of S2 in both solutions were smaller than that in solvent alone (pure water). This means that some water molecules interacted with the samples to result in the formation of S1 at 30 °C (Sekiguchi, Sawatari, & Kondo, 2001).

At 90 °C where the gelation of R-MC and 2,3MC-1b solutions was observed, the area of S0 of water increased, whereas the area of S2 of water decreased. Because of the breaking of some hydrogen bonds in the water structure at higher temperature, the resulting water molecules may be altered to the free states (S0) (Bujis & Choppin, 1963). The areas of S1 in both 2,3MC-1b and R-MC solutions were larger than that in solvent alone (pure water) at 90 °C. This indicates that the intermolecular hydrogen bonds between water and the samples are present at high temperatures.

The area of S1 of water in the 2,3MC-1b solution was slightly larger than that in R-MC solution at 90 °C. In 2,3MC-*n* samples, methyl groups at the C(2) and C(3) positions are almost unable to form three-dimensional networks by themselves, but are sterically able to form the intermolecular hydrogen bonds with hydroxyl groups at the C(6) position, leading to crosslinking networks. Thus in *O*-methylcellulose/water system, gel formation is caused by the hydrophobic interaction as well as the intermolecular hydrogen bonds. These phenomena were also shown in the gelation of 2,3-di-*O*-benzylcellulose in tetrahydrofuran (Itagaki et al., 1994, 1997). The main cause for the gelation was the hydrogen bonds with hydroxyl groups at the C(6) position, whereas the hydrophobic interaction between benzyl groups also kept 2,3-di-*O*-benzylcellulose molecules associated with one other.

The superstructure of aggregated states for R-MC and 2,3MC-1b solutions were investigated using SAXS. The reflection was observed from $2\theta = 0.3$ ($d = 288$ Å) to 1.2° ($d = 72$ Å) in SAXS patterns for R-MC and from $2\theta = 0.4$ ($d = 215$ Å) to 1.6° ($d = 54$ Å) for 2,3MC-1b solutions, respectively (shown in Fig. 8). This indicates that the reflection corresponds to the gel structures aggregated in these solutions and yet the gel structures have an irregular size: in R-MC, the intensity of the reflection at $2\theta = 0.4$ ($d = 215$ Å) increased after 40 min. Because the main cause for the gel formation in R-MC solution is the hydrophobic interaction among trimethyl glucose sequences, the number of crosslinking networks may increase. In 2,3MC-1b, the intensity of the reflection at $2\theta = 0.7$ ($d = 123$ Å) slightly increased with the measuring time. This means that the crosslinking networks, which were formed by the intermolecular hydrogen bonds with hydroxyl groups prior to the gelation, are not able to grow sterically. Therefore, it indicates that the growth of crosslinking junction may be dependent on the hydrophobic interaction in the gels.

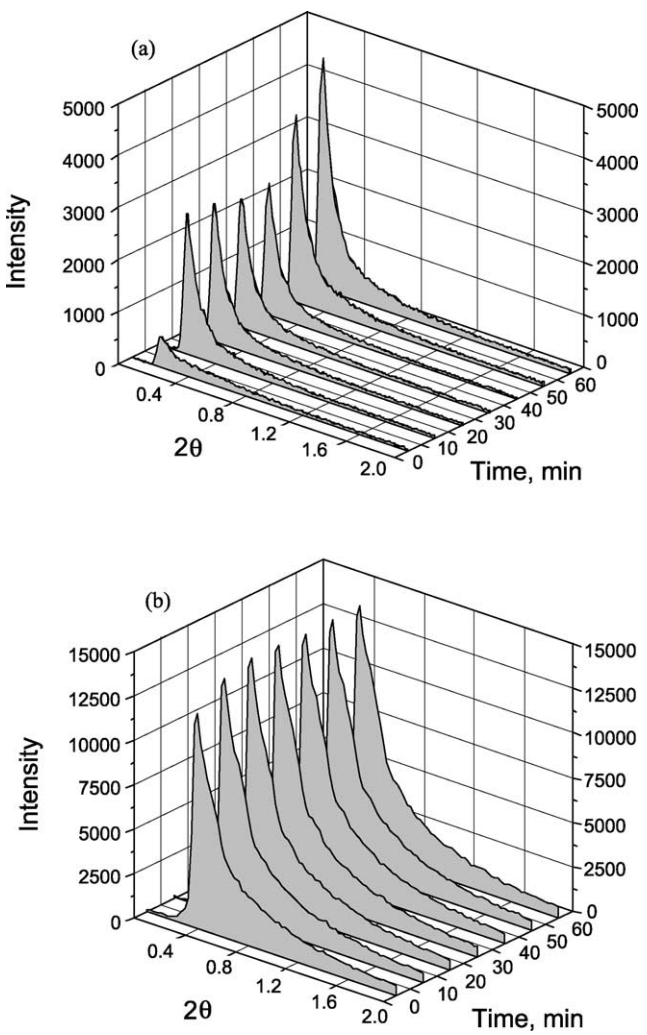

Fig. 8. SAXS pattern by synchrotron radiation of (a) 2 wt% R-MC and (b) 25 wt% 2,3MC-1b solutions at 65 °C.

4. Conclusion

The gel formation of the 2,3MC-*n* samples and R-MC in aqueous solution was investigated in this research. The distribution of the unsubstituted hydroxyl groups in 2,3MC-*n* cast films were calculated from the area of OH stretching bands in IR spectra. In 2,3MC-*n* series, gelation was dependent on the flexibility of the cellulose molecular chains restrained by the intramolecular hydrogen bonds. 2,3MC-*n* samples having fewer intramolecular hydrogen bonds in solutions are prone to form gels on heating.

Three solutions from 2,3MC-*n*b series as well as R-MC solution formed gels. The concentration of 2,3MC-*n*b series necessary to form a gel was between 20 and 25 wt%, whereas that of R-MC was between 1 and 5 wt%. The DSC thermograms of the 2,3MC-*n* solutions in the heating scan showed monotonic endothermic curves, whereas that of R-MC showed two endothermic peaks. These results suggest that the gelation mechanism of 2,3MC-*n*b samples may involve other interactions differing from the hydrophobic interaction as seen in R-MC solution.

The OH stretching region of water in NIR spectra of the sample solutions was composed of water species involving 0, 1, and 2 hydrogen bonds per molecules (S0, S1, and S2), respectively. The area of S1 of water in 2,3MC-1b solution was larger than that in solvent alone (pure water), and were slightly larger than that in R-MC solution at 90 °C where the gelation of R-MC and 2,3MC-1b solutions was observed. This indicates the presence of intermolecular hydrogen bonds between the sample and water. 2,3MC-1b gel is considered to form intermolecular hydrogen bonds with hydroxyl groups at the C(6) position, because methyl groups at the C(2) and C(3) positions are almost unable to form three-dimensional networks. The gel formation of 2,3MC-1b solution presented here can also explain why there is no increase in the intensity of the reflection at $2\theta = 0.7$ ($d = 123$ Å) in SAXS pattern.

Acknowledgements

The authors are indebted to Prof. S. Katayama, Shizuoka Prefecture University, for the micro DSC, and Prof. G. Okada, T. Asano, Shizuoka University, for the use of HPLC, SAXS. We also thank Dr Dwight Romanovicz at the University of Texas at Austin for editing the text.

References

Buijs, K., & Choppin, G. R. (1963). Near infrared studies of the structure of water. I. Pure water. *Journal of Chemical Physics*, *39*, 2035–2041.

Founés, V., & Chaussidon, J. (1978). An interpretation of the evolution with temperature of the $\nu_2 + \nu_3$ combination band in water. *Journal of Chemical Physics*, *68*, 4667–4671.

Hirren, M., Chevillard, C., Desbrières, J., Axelose, M. A. V., & Rinaudo, M. (1998). Thermogelation of methylcelluloses: New evidence for understanding the gelation mechanism. *Polymer*, *39*, 6251–6259.

Hirren, M., Desbrières, J., & Rinaudo, M. (1997). Physical properties of methylcellulose in relation with the conditions for cellulose modification: New evidence for understanding the gelation mechanism. *Carbohydrate Polymers*, *31*, 243–252.

Itagaki, H., Takahashi, I., Natsume, M., & Kondo, T. (1994). Gelation of cellulose whose hydroxyl groups are specifically substituted by the fluorescent groups. *Polymer Bulletin*, *32*, 77–81.

Itagaki, H., Tokai, M., & Kondo, T. (1997). Physical gelation for cellulose whose hydroxyl groups are regioselectively substituted by the fluorescent groups. *Polymer*, *38*, 4201–4205.

Kato, T., Yokoyama, M., & Takahashi, A. (1978). Melting temperature of thermally reversible gels IV. Methyl cellulose–water gels. *Colloid and Polymer Science*, *256*, 15–21.

Kondo, T. (1993). Preparation of 6-*O*-alkylcelluloses. *Carbohydrate Research*, *238*, 231–240.

Kondo, T. (1994). Hydrogen bonds in regioselectively substituted cellulose derivatives. *Journal of Polymer Science B: Polymer Physics*, *32*, 1229–1236.

Kondo, T. (1997a). The relationship between intramolecular hydrogen bonds and certain physical properties of regioselectively substituted cellulose derivatives. *Journal of Polymer Science B: Polymer Physics*, *35*, 717–723.

Kondo, T. (1997b). The assignment of IR absorption bands due to free hydroxyl groups in cellulose. *Cellulose*, *4*, 281–292.

Kondo, T., & Gray, D. G. (1991). The preparation of *O*-methyl- and *O*-ethyl-celluloses having controlled distribution of substituents. *Carbohydrate Research*, *220*, 173–183.

Kondo, T., & Gray, D. G. (1992). Facile method for the preparation of tri-*O*-(alkyl)cellulose. *Journal of Applied Polymer Science*, *45*, 417–423.

Kondo, T., & Miyamoto, T. (1998). The influence of intramolecular hydrogen bonds on handedness in ethylcellulose/CH_2Cl_2 liquid crystalline mesophases. *Polymer*, *39*, 1123–1127.

Kondo, T., & Nojiri, M. (1994). Characterization of the cleavage of β-glucosidic linkage by *Trichoderma viride* cellulase using regioselectively substituted methylcellulose. *Chemistry Letters*, 1003–1006.

Liu, H. Q., Zhang, L. N., Takaragi, A., & Miyamoto, T. (1997). A further study on water solubility of *O*-methylcellulose. *Cellulose*, *4*, 321–328.

McCabe, W. C., & Fisher, H. F. (1965). Measurement of the excluded volume of protein molecules by differential spectroscopy in near infrared. *Nature*, *207*, 1274–1276.

McCabe, W. C., & Fisher, H. F. (1970). A near infra-red spectroscopic method for investigating the hydration of a solute in aqueous solution. *Journal of Physical Chemistry*, *74*, 2990–2998.

Nishimura, H., Donkai, N., & Miyamoto, T. (1997). Temperature-responsive hydrogels from cellulose. *Macromolecules Symposium*, *120*, 303–308.

Nojiri, M., & Kondo, T. (1996). Application of regioselectively substituted methylcelluloses to characterize the reaction mechanism of cellulase. *Macromolecules*, *29*, 2392–2395.

Sarkar, N. (1979). Thermal gelation properties of methyl and hydroxypropyl methylcellulose. *Journal of Applied Polymer Science*, *24*, 1073–1087.

Sarkar, N. (1995). Kinetics of thermal gelation methylcellulose and hydroxypropyl methylcellulose in aqueous solutions. *Carbohydrate Polymers*, *26*, 195–203.

Sekiguchi, Y., Sawatari, C., & Kondo, T. (2001). Characterization of hydrogen bonds in *O*-methylcellulose/dimethyl sulfoxide/water system by FT-NIR analysis. *Reports of The Graduate School of Electronic Science and Technology Shizuoka University*, *22*, 19–24.

Sekiguchi, Y., Sawatari, C., & Kondo, T. (2002). A facile method of determination for distribution of the substituent in *O*-methylcelluloses using ^{1}H-NMR spectroscopy. *Polymer Bulletin*, *47*, 547–554.

Suzuki, K., Taniguchi, Y., & Enomoto, T. (1972). The effects of pressure on the sol–gel transformations of macromolecules. *Bulletin of the Chemical Society Japan*, *45*, 336–338.

Takaragi, S., Fujimoto, T., Miyamoto, T., & Inagaki, H. (1987). Relationship between distribution of substituents and water solubility of *O*-methyl cellulose. *Journal of Polymer Science A: Polymer Chemistry*, *25*, 987–994.

Vigouret, M., Rinaudo, M., & Desbrières, J. (1996). Thermogelation of methylcellulose in aqueous solution. *Journal of Chemical Physics*, *93*, 858–869.